HHS Public Access

Author manuscript

Cell Chem Biol. Author manuscript; available in PMC 2021 April 17.

Published in final edited form as:

Cell Chem Biol. 2020 October 15; 27(10): 1229–1240.e4. doi:10.1016/j.chembiol.2020.07.011.

Chemical Biology Toolkit for DCLK1 Reveals Connection to RNA Processing

Yan Liu[1,2], **Fleur M. Ferguson**[3,4], **Lianbo Li**[1,2], **Miljan Kuljanin**[5], **Caitlin E. Mills**[6], **Kartik Subramanian**[6,7], **Wayne Harshbarger**[1,2], **Sudershan Gondi**[1,2], **Jinhua Wang**[3,4], **Peter K. Sorger**[6], **Joseph D. Mancias**[5], **Nathanael S. Gray**[3,4], **Kenneth D. Westover**[1,2,8,*]

[1]Department of Biochemistry, The University of Texas Southwestern Medical Center at Dallas, Dallas, TX 75390, USA

[2]Department of Radiation Oncology, The University of Texas Southwestern Medical Center at Dallas, Dallas, TX 75390, USA

[3]Department of Cancer Biology, Dana-Farber Cancer Institute, Boston, MA 02215, USA

[4]Department of Biological Chemistry and Molecular Pharmacology, Harvard Medical School, Boston, MA 02115, USA

[5]Division of Radiation and Genome Stability, Department of Radiation Oncology, Dana-Farber Cancer Institute, Boston, MA 02115, USA

[6]Laboratory of Systems Pharmacology, Department of Systems Biology, Harvard Program in Therapeutic Science, Harvard Medical School, Boston, MA 02115, USA

[7]Present address: Bristol-Myers Squibb, 100 Binney St, Cambridge, MA 02142, USA

[8]Lead Contact

SUMMARY

Doublecortin-like kinase 1 (DCLK1) is critical for neurogenesis, but overexpression is also observed in multiple cancers and is associated with poor prognosis. Nevertheless, the function of DCLK1 in cancer, especially the context-dependent functions, are poorly understood. We present a

*Correspondence: kenneth.westover@utsouthwestern.edu.

AUTHOR CONTRIBUTIONS

K.D.W. and Y.L. conceived and led the study. Y.L., F.M.F., J.D.M., L.L., M.K., W.H., S.G., J.W., C.E.M., K.S., P.K.S., N.S.G., and W.H. designed and conducted the experiments, analyzed and interpreted the data. J.D.M., K.D.W., and N.S.G. supervised aspects of the project. K.D.W. and Y.L. wrote the manuscript, with edits from F.M.F., J.D.M, and N.S.G. All authors read and approved the manuscript.

DECLARATION OF INTERESTS

F.M.F. and N.S.G. are inventors on a patent application related to the DCLK1 inhibitors described in this manuscript (WO/2018/075608). K.D.W. has received consulting fees from Sanofi Oncology and is a member of the SAB for Vibliome Therapeutics. K.D.W. declares that none of these relationships are directly or indirectly related to the content of this manuscript. N.S.G. is a Scientific Founder, member of the SAB, and equity holder in C4 Therapeutics, Syros, Soltego (board member), B2S, Aduro Gatekeeper, and Petra Pharmaceuticals. The Gray lab receives or has received research funding from Novartis, Takeda, Astellas, Taiho, Janssen, Kinogen, Voroni, Her2llc, Deerfield, and Sanofi. P.K.S. is a member of the SAB or Board of Directors of Applied Bio-math and RareCyte, Inc., and has equity in these companies. P.K.S. has received research funding from Novartis and Merck in the last 5 years. P.K.S. declares that none of these relationships are directly or indirectly related to the content of this manuscript. P.K.S. is a current employee of Bristol-Myers Squibb.

SUPPLEMENTAL INFORMATION

Supplemental Information can be found online at https://doi.org/10.1016/j.chembiol.2020.07.011.

"toolkit" that includes the DCLK1 inhibitor DCLK1-IN-1, a complementary DCLK1-IN-1-resistant mutation G532A, and kinase dead mutants D511N and D533N, which can be used to investigate signaling pathways regulated by DCLK1. Using a cancer cell line engineered to be DCLK1 dependent for growth and cell migration, we show that this toolkit can be used to discover associations between DCLK1 kinase activity and biological processes. In particular, we show an association between DCLK1 and RNA processing, including the identification of CDK11 as a potential substrate of DCLK1 using phosphoproteomics.

In Brief

DCLK1 overexpression occurs in cancer, suggesting that DCLK1 is a therapeutic target. We report a tool kit for the study of DCLK1, including engineered DCLK1-dependent cancer cells, a DCLK1 inhibitor, and DCLK1 mutations that ablate kinase activity or confer drug resistance. We found a new association between DCLK1 and RNA processing.

Graphical Abstract

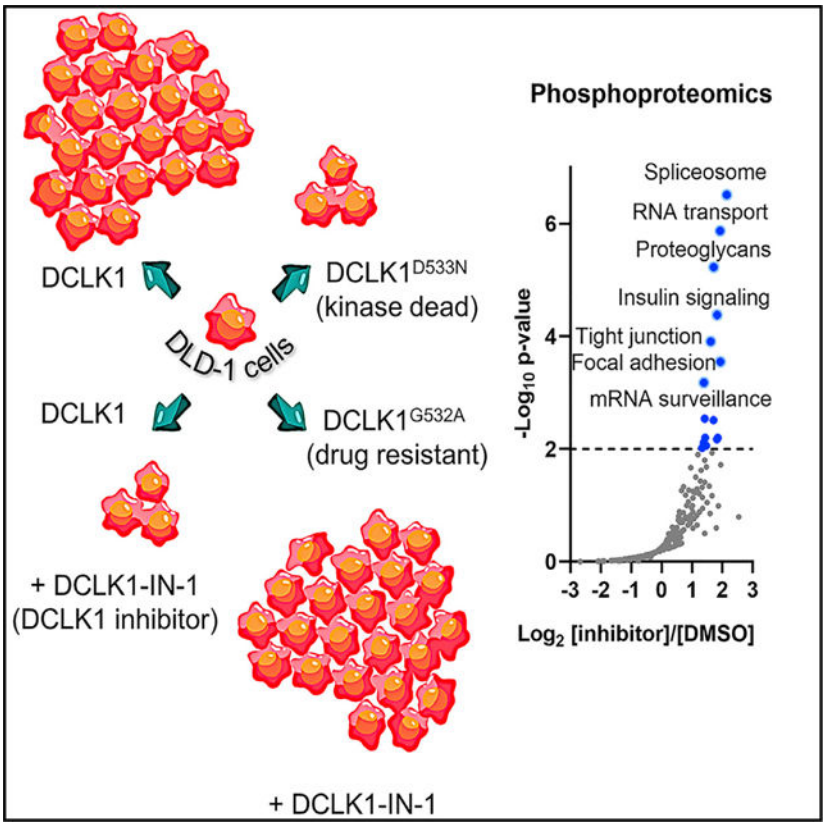

INTRODUCTION

Doublecortin-like kinase 1 (DCLK1) is a multi-domain protein belonging to both the doublecortin (DCX) and the protein kinase super families (Reiner et al., 2006). DCLK1 was originally identified in post-mitotic neurons as a regulator of microtubule polymerization in migrating neurons (Koizumi et al., 2017; Lin et al., 2000; Lipka et al., 2016; Qu et al., 2014;

Sossey-Alaoui and Srivastava, 1999). Subsequent work established roles for DCLK1 in neuronal migration, neurogenesis, retrograde transport, and neuronal apoptosis (Liu et al., 2012; Mizuguchi et al., 1999; Verissimo et al., 2010). However, DCLK1 is also implicated in human cancers. Whole-genome sequencing of human gastric tumors has identified frequent somatic missense mutations in DCLK1, with mutations found in ~10% of tumors (Cancer Genome Atlas Research, 2014). DCLK1 is also upregulated in cancers of the skin, colon, pancreas, liver, esophagus, kidney, and small intestine (Gao et al., 2016; Ito et al., 2016; Sakaguchi et al., 2016; Chandrakesan et al., 2017; Ikezono et al., 2017; Wang et al., 2016; Westphalen et al., 2016; Weygant et al., 2016; Kadletz et al., 2017) and can be significantly increased in later-stage disease (Weygant et al., 2015). Elevated expression of DCLK1 is also associated with cancer-specific mortality in colon and gastric cancer (Gagliardi et al., 2012; Wu et al., 2020).

Several DCLK1-mediated cancer mechanisms have been reported (Cancer Genome Atlas Research, 2014; Wang et al., 2014; Weygant et al., 2016). In pancreatic and colorectal cancers (CRCs), DCLK1 promotes tumor initiation and is a marker of cancer stem cells (Bailey et al., 2014; Chandrakesan et al., 2014, 2015, 2016; Gao et al., 2016; Ito et al., 2016; Koga et al., 2016; Nakanishi et al., 2013; Sakaguchi et al., 2016; Vedeld et al., 2014; Westphalen et al., 2016). In a subset of colon and lung cancers, DCLK1 also causes chromosomal instability and impairs DNA repair in a kinase and microtubule binding-independent manner (Lu et al., 2018). In neuroblastoma cell lines, the microtubule binding function of DCLK1 modulated responses to microtubule-disrupting drugs (Verissimo et al., 2012). DCLK1 has also been identified as a potential RAS effector (Westphalen et al., 2016). Given the multi-faceted nature of DCLK1 function, convenient research tools focused on DCLK1 function are needed to clarify its roles in cancer and to determine which of those constitute a bona fide vulnerability for cancer therapy.

It is well established that the kinase domain of DCLK1 is druggable (Deng et al., 2011a; Powrozek et al., 2016; Suehiro et al., 2018; Sureban et al., 2013, 2014, 2015; Wang et al., 2016; Westphalen et al., 2017; Weygant et al., 2014, 2015; Whorton et al., 2015). Multi-targeted probes such as LRRK2-IN-1 and XMD892, which share a benzo[e]pyrimido scaffold, have been used to study the effects of DCLK1 inhibition (Deng et al., 2011b; Lenart et al., 2007; Steegmaier et al., 2007) and have shown anti-tumor effects in pancreatic cancer models (Sureban et al., 2014; Weygant et al., 2014). Nevertheless, the multi-targeted nature of these compounds leaves open the possibility that phenotypes are from off-target effects.

Recently the X-ray structure of DCLK1 became available, making possible structure-guided optimization of the benzo[e] pyrimido scaffold in favor of DCLK1 (Patel et al., 2016). A paucity of side-chain volume in the back pocket of DCLK1 raised the possibility of improving compound selectivity by adding substituents that occupy that pocket. Indeed, addition of a trifluoro substituent resulted in improved selectivity for DCLK1 for the compound DCLK-IN-1 (Ferguson et al., 2020). Here we report further characterization of DCLK1-IN-1 and the discovery of complementary DCLK1 mutations, including kinase dead (KD) and drug-resistance mutations and demonstrate their utility in studying the CRC cell line DLD-1. This same suite of tools may be applied to other cancer models to clarify the

roles of DCLK1 and discover predictive biomarkers to direct patient selection for DCLK1-directed cancer therapies.

RESULTS

DCLK1 Kinase Activity Is Required for DLD-1 Growth and Invasion

The DCLK1 small-molecule inhibitor, DCLK1-IN-1, and the negative control, DCLK1-NEG, are generally non-toxic for cell growth (Figure S1) and predictive biomarkers of anti-proliferative effects of DCLK1-IN-1 are currently not established. Therefore, we sought to develop a cellular system through genetic means that was DCLK1 dependent for growth. The structure of DCLK1 suggests that Lys 419, Asp 511, Asn 516, and Asp 533 are involved in catalysis (Figures 1A and S2) (Patel et al., 2016). This predicts that DCLK1 D511N and D533N mutations will abolish kinase activity. These mutant proteins were recombinantly expressed and purified from *E. coli*. They exhibited no kinase activity in peptide substrate mobility shift biochemical enzyme assays, as expected (Figure 1B). We overexpressed DCLK1 or DCLK1-KD D511N mutant or D533N mutant in DLD-1 cells. All DCLK1 expression constructs showed similar levels of DCLK1 by western blot (Figure S3). Wild-type (WT) expression in DLD-1 cells had no effect on cell proliferation compared with a GFP control; however, expression of DCLK1-KD reduced cell growth (Figure 1C). Similar effects were observed in cell invasion (Figure 1D) and colony-formation assays (Figure 1E). Because DCLK1 has been reported as a cancer stem cell marker in CRC and plays an important role in CRC tumorigenesis (Mohammadi et al., 2018; Nakanishi et al., 2013), we evaluated whether overexpression of DCLK1 or DCLK1-KD could alter spheroid formation of CRC cells, a defining feature of cancer stem cells *in vitro* (Shaheen et al., 2016). DCLK1 overexpression significantly increased the sphere volume, but DCLK1-KD dramatically reduced the sphere volume of DLD-1 cells (Figures 1F and 1G). This establishes that DLD-1 cells are dependent on DCLK1 kinase activity for spheroid growth of DLD-1 cells and that both Asp 511 and Asp 533 are required for DCLK1 kinase activity.

DCLK1-IN-1 Phenocopies DCLK-1-KD

DCLK1-IN-1 (Figure 2A) is a highly selective, ATP-competitive inhibitor of DCLK1 kinase activity (Ferguson et al., 2020). To show that DCLK1-IN-1 can engage with DCLK1 specifically in DLD-1 cells, we performed a cellular thermal shift assay to evaluate drug target interactions (Jafari et al., 2014). In this assay, the ability of compounds to enhance the thermal stability of proteins in cells indicates target engagement. We treated DLD-1 cells overexpressing DCLK1 with 1 μM DCLK1-IN-1 overnight, collected the cells, and exposed these to a temperature gradient. DCLK1-IN-1 treatment increased the levels of soluble DCLK1 in cells by approximately 3°C compared with DMSO or treatment with 1 μM DCLK1-NEG, which incorporates a methyl group that prevents DCLK1 binding (Figures 2B and S4) (Ferguson et al., 2020), confirming that DCLK1-IN-1 binds to DCLK1 in DLD-1 cells.

Having confirmed target engagement of DCLK1 by DCLK-IN-1 in DLD-1 cells, we directly compared the phenotype of DCLK1-IN-1 treatment with genetic abolishment of DCLK1 kinase function. In 2D culture, DCLK1-IN-1 reduced cell proliferation of DLD-1 cells

overexpressing WT DCLK1 in a dose-dependent manner (Figure 2C left panel), while DCLK1-NEG showed no effects (Figure 2C right panel). Similarly, DCLK1-IN-1 decreased colony formation (Figure 2D) and cell invasion (Figure 2E). DCLK1-IN-1 also abolished spheroid formation (Figures 2F and 2G), consistent with the genetic DCLK-KD phenotype. This establishes that DCLK1-IN-1 phenocopies the KD version of DCLK1 for DLD-1 cell growth, invasion and spheroid formation.

DCLK1 G532A Is Resistant to DCLK1-IN-1 Treatment

Acquired resistance occurs commonly in response to targeted cancer therapies and is often caused by mutations in a drug binding site that prevent binding (Hoelder et al., 2012). An analogous concept has been used in chemical biology studies as a control to demonstrate the on-target effects of small-molecule inhibitors (Lim et al., 2015; Xie et al., 2014). We aimed to generate a DCLK1-IN-1-resistant version of DCLK1. Recently several crystal structures of DCLK1 became available, including a structure of DCLK1 bound to NVP-TAE684 (PDB: 5JZN; Patel et al., 2016). In addition, several co-structures of kinases bound to compounds containing the benzo[e]pyrimido scaffold have also become available, including the structure of CHK1 (PDB: 5OQ5; Williamson et al., 2017), ERK5 (PDB: 5BYY; Chen et al., 2016), ROCO4 (PDB: 4YZM; Gilsbach et al., 2015), and AURK (PDB: 3ZTX; Ferguson et al., 2017). All of these structures show a similar binding mode. Using the available DCLK1 kinase structure, we performed an unconstrained, induced fit docking of DCLK1-IN-1. The resulting pose was highly similar to binding modes seen in previously solved crystal structures of benzo[e]pyrimido scaffolds (Figure 3A). In this model DCLK1 residues L440, V449, and G532 form van der Waals interactions with the trifluoroethyl portion of DCLK1-IN-1 to DCLK1 protein. We compared these side chains with those found in other known targets of benzo[e] pyrimido scaffolds, including AURK, CHK1, ERK5, and ROCO4, which do not bind to DCLK1-IN-1. We noted that the side chains in DCLK1 surrounding the trifluoro contained comparatively fewer atoms than other potential off-targets. We computed the side-chain volumes (Baumann et al., 1989; Richards, 1977) and found that DCLK1 had the smallest side-chain volume (Figure 3B). This is consistent with the original design concept of DCLK1-IN-1, which hypothesized that selectivity could arise from clashes between the trifluoro substituent and some combination of side chains at positions equivalent to DCLK1 L440, V449, and G532 (Figure 3A) (Ferguson et al., 2020). We considered that introduction of additional side-chain volume into the trifluoro binding pocket of DCLK1 would result in a DCLK1-IN-1-resistant mutant. We searched the kinome for tolerated substitutions at the equivalent position of G532 in DCLK1 and found that other kinases have Ala, Ser, or Val at this position. We expressed and purified DCLK1 with G532A, G532S, and G532V. Of these, only G532A had the same level of kinase activity as DCLK1 WT in the enzymatic assay (Figure 3C). To confirm that G532A mutation prevents DCLK1-IN-1 binding, we used isothermal titration calorimetry (ITC) to characterize the binding affinity between DCLK1-IN-1 and DCLK1 G532A. Previous studies suggested the binding constant (K_d) of DCLK1-IN-1 and DCLK1 is 109 nM (Ferguson et al., 2020). However, no binding was detected with DCLK1 G532A protein (Figure 3D). We further showed drug resistance by measurement of kinase activity using purified DCLK1 G532A protein. DCLK1-IN-1 showed no inhibitory effects on the activity of DCLK1 G532A,

whereas DCLK1-IN-1 inhibited DCLK1 WT with a half maximal inhibitory concentration of 55 nm (Figure 3E).

We characterized the DCLK1 G532A in DLD-1 cells. Cells overexpressing WT DCLK1 or DCLK1 G532A showed no difference in cell growth (Figure 4A), suggesting equivalence in the biological function of these DCLK1 forms. However, DCLK1 G532A-bearing cells were completely resistant to treatment by DCLK1-IN-1 in cell proliferation assays (Figure 4B), cell invasion (Figure 4C), colony formation (Figure 4D), and spheroid formation assays (Figures 4E and 4F). The ability of the DCLK1 G532A mutation to rescue from DCLK1-IN-1-dependent phenotypes confirms that these phenotypes are due to on-target inhibition of DCLK1. This establishes that DCLK1 G532A is resistant to inhibition by DCLK1-IN-1 and that the G532A substitution can be used to establish DCLK1 on-target effects via rescue experiments of DCLK1-IN-1-dependent phenotypes.

Perturbation of the Phosphoproteome in Colon Cancer Cells by DCLK1-IN-1

Selective DCLK1 inhibitors provide an opportunity to discover new aspects of DCLK1 biology such as downstream signaling pathways. To show the utility of DCLK1-IN-1 in elucidating DCLK1-related signaling in colon cancer, we conducted a time-dependent phosphoproteomics analysis of DCLK1-overexpressing DLD-1 cell lines after treatment with DCLK1-IN-1. In these experiments, cells were grown to confluency, treated with 1 mM of DCLK1-IN-1 for the indicated times, and then harvested and processed using quantitative phosphoproteomics as described previously (Lyons et al., 2018). The DCLK1-IN-1 treatment resulted in minor changes in the proteome overall; however, we did observe time-dependent changes in the phosphoproteome (Figure 5A).

We first evaluated for significantly downregulated phosphopeptides, which could be potential direct or indirect substrates of DCLK1. We found that phosphopeptides from TOP2B, CDK11B, and MATR3 showed marked depletion at 1, 4, and 24 h post-treatment (Table 1). To confirm that this was not related to changes in the protein levels, we confirmed by normalizing to the proteome at each time point (Figure 5B). DCLK1-dependent phosphorylation of these substrates has not been reported previously.

We next analyzed for enrichment or depletion of biologically related phosphopeptides ($p < 0.05$) using Kyoto Encyclopedia of Genes and Genomes analysis. At early time points there were coordinated changes in phosphopeptides from proteins involved in RNA processing, insulin signaling, ErbB signaling, proteoglycan synthesis, and maintenance of focal adhesion and tight junction pathways (Figures 5C and S5). Of these, changes in RNA processing and proteoglycan-related genes persisted at 24 h. Finally we performed analysis of kinase activity by inference, given that DCLK1 has been shown to act, at some level, through kinase-mediated signaling networks (Ikezono et al., 2017; Liu et al., 2018; Rangarajan et al., 2015). Kinase activity was inferred by performing GSEA analysis of phosphorylation levels for custom protein sets that are known substrates of kinases, similar to previous analyses (Poulin et al., 2019). Multiple kinases showed significant changes in inferred activity based on enrichment or depletion of peptide substrates at various time points (false discovery rate <0.25; Figure 5D), including CDK1/2, ERK2, GSK3B, CHK1, and PKACA (Figure S6). This finding is consistent with the DCLK1-IN-1-induced phenotype in DLD-1 cells, given

that all of these pathways are important for cell migration and proliferation; phenotypes for which these DLD-1 cells are DCLK1 dependent. In summary, the phosphoproteomics analysis establishes that DCLK1-IN-1 can be used as a discovery tool to identify substrates and biological processes that rely on DCLK1 function.

DISCUSSION

Here, we report a set of chemical and genetic tools for the study of DCLK1, including the KD mutations D511N and D533N, drug-resistance mutation G532A for the selective DCLK1 inhibitor DCLK1-IN-1, and an engineered DCLK1-dependent cancer cell line. Both DCLK1-KD and DCLK1-IN-1 treatment produced similar phenotypes in the DLD-1 model line. These phenotypes were fully reversed by the resistant mutation G532A, confirming that effects seen after DCLK1-IN-1 exposure are DCLK1 dependent. DCLK1-IN-1 also enabled identification of substrates of DCLK1 and an association of DCLK1 activity with RNA processing. Altogether, this work establishes a set of DCLK1 inhibitors and complementary mutations that can be used as a toolkit for examining the functions of DCLK1 in various contexts and for evaluating prospective DCLK1-targeted therapies.

From this work it is unclear exactly how KD versions of DCLK1 produce a dominant negative phenotype in DCLK1, but presumably this is related to the ability to out-compete the endogenous active enzyme. Given that, DCLK1 includes DCX domains that bind to microtubules, one possibility is that DCLK1 -KD displaces active DCLK1 at the microtubules and exerts its effects in this manner. Additional work on this area may clarify the apparent connection between DCLK1 kinase activity and the function of the DCX domains.

A future goal is to explain the functions of DCLK1 in cancer, which appear to be variable and context dependent (Sureban et al., 2015). We showed that DCLK1-IN-1 can be used to identify the underlying signaling pathways that DCLK1 utilizes to regulate cell growth and migration, in DLD-1 cells, including RNA-related pathways, insulin signaling and proteoglycan, focal adhesion and tight junction pathways. Association of focal adhesion and tight junction pathways with DCLK1 is consistent with previous reports showing that focal adhesion becomes dysregulated in cancer cell lines in a DCLK1-dependent manner leading to epithelial-to-mesenchymal transition (Weygant et al., 2015). It is also consistent with the observation that DCLK1 knockout mice lose their ability to maintain tight junctions (May et al., 2014). However, to our knowledge DCLK1 has not been associated with RNA trafficking/processing and insulin signaling/proteoglycans prior to this study.

In addition, our GSEA analysis of kinase activity identified ERK2, GSK3B, CDK1, CDK2, CHK1, and PKACA activity as affected by DCLK1 inhibition. Some of these findings are compatible with previous reports that DCLK1 interacts with SRC leading to activation of FAK, which phosphorylates ERK and upregulates cyclin D1 leading to cell migration and proliferation (Ikezono et al., 2017). However, a regulatory link between DCLK1 and PKACA or GSK3B has not been reported previously. Confirming this link, and the significance thereof, will be the subject of future efforts.

Our analysis also associated DCLK1 with several potential substrates involved in nucleic acid processing, including CDK11, MATR3, and DNA topoisomerase 2-beta (*TOP2B*). The sites in which we identify a decrease in response to DCLK1-IN-1 are likely DCLK1 substrates given the high selectivity of DCLK1-IN-1, but there is a possibility for off-target effects. Indeed, our novel mutants will aid in the discovery of DCLK1-IN-1 on- and off-target substrates in future phosphoproteomic studies. CDK11 is a serine/threonine protein kinase in the CDK family, which forms a complex with the cyclin L regulatory partner and plays a role in pre-mRNA splicing (Hu et al., 2003). Overexpression of CDK11 has been detected in human cancers and inhibition or deletion of CDK11 in cancer cells leads to cancer cell death and apoptosis (Lin et al., 2019). CDK11 null cells also display defects in cell growth, mitotic arrest, and apoptosis. Therefore, CDK11 is considered a therapeutic target (Ahmed et al., 2019; Zhou et al., 2015, 2016), but has been difficult to selectively inhibit with small molecules. It may be possible to exploit the connection between DCLK1 and CDK11 to target CDK11-dependent disease processes.

MATR3 encodes a nuclear matrix protein, which binds to DNA and RNA, playing roles in RNA processing and mRNA stabilization (Johnson et al., 2014; Salton et al., 2011). Under normal physiological conditions, both MATR3 and DCLK1 are detected in neuronal cells (Malik et al., 2018; Shin et al., 2013), supporting the idea that DCLK1 could regulate MATR3 in neurons. However, the role of MATR3 in cancer is less clear.

TOP2B encodes a type II topoisomerase, an essential gene (Yang, 2000) that functions to make transient double-stranded DNA breaks during DNA replication and gene transcription (Austin and Marsh, 1998). Top2β is expressed in all mammalian cells throughout the cell cycle and is essential to the survival of proliferating cells (Lyu and Wang, 2003; McClendon and Osheroff, 2007). It has therefore been exploited as a cancer target to treat numerous human malignancies, although topoisomerase inhibitors can produce significant toxicity (McClendon and Osheroff, 2007). If DCLK1 is confirmed as a regulator of Top2β in cancer cells, this could create opportunities for potentially less toxic treatment of cancer.

Finally, while DCLK1 overexpression has been considered a potential marker of DCLK1-dependent tumors, this concept has not yet borne out. Chemical probes are powerful tools for subtyping the heterogeneity of cancer and for the discovery of “therapeutic triads,” defined as the combination of a target, an inhibitor, and an enrollment biomarker (McMillan et al., 2018). Now that DCLK1 inhibitors have been developed, they can enable discovery of predictive biomarkers of response. We anticipate that these data and data provided in Ferguson et al. (2020) will help to guide such endeavors. Specifically, given the K_d of ~100 nM as measured by ITC, target engagement in cells of ~280 nM as measured by nano-BRET, and excellent kinome selectivity at 2.5 μM as measured by KiNativ, we anticipate that working with concentrations of ~1 μM of DCLK1-IN-1 will be effective for cell-based studies.

In summary, multiple lines of evidence suggest there is value in inhibiting DCLK1 as a cancer therapy. The genetic and chemical tools reported here will hasten progress in understanding DCLK1 cancer biology and identifying appropriate populations for the application of this therapeutic concept.

SIGNIFICANCE

DCLK1 was originally identified a regulator of microtubule polymerization in migrating neurons but has also emerged as a potential driver of human cancers. How DCLK1 functions as an oncogene in each of these contexts and whether it is a targetable vulnerability for cancer therapy are unclear. Here, we report a set of chemical biology tools to enable studies of DCLK1 function, with an emphasis on kinase inhibition. We demonstrate that kinase dead versions of DCLK1, D511N, and D533N, are dominant negative with respect to several cell growth and invasion phenotypes in the colon cancer cell line DLD-1. This phenotype is most apparent in three-dimensional culture. The selective DCLK1 small-molecule inhibitor DCLK1-IN-1 recapitulates these phenotypes but the analog DCLK1-NEG does not. To further establish that the DCLK1-IN-1-dependent phenotype is on-target for DCLK1, we developed a drug-resistance mutant, DCLK1 G532A, that prevents compound binding and rescues cells from DCLK1-IN-1 treatment. We used DCLK1-IN-1 in combination with phosphoproteomics to discern potential DCLK1-dependent pathways that support DLD-1 growth and to discover substrates of DCLK1 such as CDK11B and additional proteins involved in RNA processing, as well as other pathways previously associated with DCLK1 activity. Our study establishes a framework to clarify the role of DCLK1 in various cancer contexts and its importance as a therapeutic target. This toolkit may also assist with understanding the function of DCLK1 in normal physiology.

STAR★METHODS

Detailed methods are provided in the online version of this paper and include the following:

RESOURCE AVAILABILITY

Lead Contact

Further information and requests for reagents and resources should be directed to and will be fulfilled by Contact Ken Westover (ken.westover@utsouthwestern.edu)

Materials Availability

All unique/stable reagents generated in this study will be provided without restriction as long as stocks remain available and reasonable compensation is provided by the requestor to cover processing and shipment.

Data and Code Availability

This study did not generate any unique datasets or code.

EXPERIMENTAL MODEL AND SUBJECT DETAILS

Cell Lines and Growth Conditions

The DLD-1 (male) cell line was obtained from the ATCC. Cells were cultured in RPMI-1640 supplemented with 10% FBS. DLD-1 stable cells expressing DCLK1 were generated by infecting of lentivirus containing DCLK1, originating from plenti6/v5 (Invitrogen), and selection using blasticidin. Single colonies were picked after 7 days of

selection with 5 mg/ml of blasticidin. Lipofectamine 2000, was used to do 293TD cell transfection and was purchased from Invitrogen. (Carlsbad, CA).

Breast cancer cell lines, 184A1 (female), 184B5 (female), AU565 (female), BT20 (female), BT474 (female), BT549 (female), CAL120 (female), CAL51 (female), CAL851 (female), CAMA1 (female), EFM19 (female), EVSAT (female), HCC1143 (female), HCC1395 (female), HCC1419 (female), HCC1569 (female), HCC1806 (female), HCC1937 (female), HCC1954 (female), HCC202 (female), HCC38 (female), HCC70 (female), HS578T (female), HTERT_HME1 (female), MCF10A (female), MCF-12A (female), MDA-MB-175-VII (female), MDA-MB-231 (female), MDA-MB-330 (female), MDA-MB-361 (female), MDA-MB-415 (female), MDA-MB-436 (female), MDA-MB-453 (female), MDA-MB-468 (female), SKBR3 (female), SUM1315 (female), SUM149 (female), SUM159 (female), SUM185PE (female), SUM229PE (female), SUM52PE (female), T47D (female), UACC-812 (female), UACC-893 (female), ZR-75-1 (female), ZR-75-30 (female), were maintained in their recommended growth conditions (see https://lincs.hms.harvard.edu/db/cells/), and seeded at the densities listed (Table S1) in 384-well Cell Carrier plates (Perkin Elmer, Waltham, MA) using a Multidrop Combi Reagent Dispenser (Thermo Fisher Scientific, Waltham, MA) and allowed to adhere to for 24 hours prior to drug treatment. Cells were treated with a half-log dilution series of the indicated drugs by pin transfer. Cells were stained and fixed for analysis at the time of drug delivery and after 72 hours of treatment. Cells were pulsed for one hour with EdU (Lumiprobe, Hunt Valley, MD) and stained with 1:2000 LIVE/DEAD Far Red Dead Cell Stain (LDR) (Thermo Fisher Scientific, Waltham, MA). Cells were then fixed with 3.7% formaldehyde (Sigma Aldrich, St. Louis, MO) for 30 minutes and permeabilized with 0.5% Triton X-100 in PBS. The EdU was labeled with cy3-azide (Lumiprobe, Hunt Valley, MD) for 30 min. The cells were then blocked for one hour with Odyssey blocking buffer (LI-COR, Lincoln, NE), and stained overnight at 4°C with 2 μg/ml Hoechst 33342 (Sigma Aldrich, St. Louis, MO) and a 1:1000 dilution of anti-phospho-histone H3 (pHH3) Alexa 488 (Ser10, clone D2C8) conjugated antibody (Cell Signaling Technologies, Danvers, MA). Fixed cells were imaged with a 10x objective using an Operetta (Perkin Elmer, Waltham, MA) or Image Xpress (Molecular Devices, San Jose, CA) microscope and analyzed using Columbus or MetaXpress software respectively. Nuclei were segmented based on their Hoechst signal, and the LDR signal was used to classify cells as live or dead. Live cell counts were normalized to DMSO-treated controls on the same plates to yield normalized growth rate inhibition (GR) values as described previously (Hafner et al., 2016). Experiments were performed as technical triplicates.

METHOD DETAILS

Plasmids, Peptide and Protein

His-tagged DCLK1 kinase domain DNA construct was a gift from Dr. Ana Clara Redondo of the Structural Genomics Consortium at the University of Oxford. DCLK1 kinase domain protein was expressed in E.coli BL21 lambda phosphatase by induction of IPTG. Cells were lysed in lysis buffer (50 mM Hepes pH 7.8, 350 mM NaCl, 20 mM Imidazole, 5% Glycerol,

5 mM β-ME) using a cell disrupter and the soluble fraction recovered by centrifugation. DCLK1 was purified using Ni-NTA resin.

DCLK1 Enzyme Activity

DCLK1 activity was measured using a peptide substrate mobility shift assay assembled from purified components. DCLK1 substrate was FL-Peptide 12 from Caliper Life Science. The sequence was 5-FAM-KKLRRTLSVA-COOH. Final reaction conditions were 3 nM DCLK1 protein, 100 mM HEPES, pH 7.5, 0.015% Brij-35, 5.0% DMSO, 0.004% Tween 20, 10 mM $MgCl_2$ and 2 mM DTT, 1 μM peptide 12, and 100 μM ATP. If inhibitors or DMSO were used, they were allowed to incubate with DCLK1 for an hour at room temperature prior to initiation of the assay by adding peptide and ATP. Endpoint assays were run for 1 hour. The reaction was quenched with 40 mM EDTA. Data was collected using a LabChip® EZ Reader (PerkinElmer) and analyzed using GraphPad.

Cellular Thermal Shift Assay

Cells were cultured in 10 cm plates and were treated with DMSO or a compound overnight. Cells were collected, washed with PBS twice. Cells were re-suspended with 1 mL of PBS and were aliquoted into 0.2 mL PCR tubes. Cells were incubated in a PCR machine for 3 minutes in a temperature gradient. Following the heating, samples were incubated at 25°C for 3 minutes. Samples were then snap-frozen in liquid nitrogen. Cell samples were frozen and thawed for three times, and were spun down at 15000 rpm for 15 minutes at 4°C. The supernatant was separated and analyzed by Western Blotting.

Isothermal Titration Calorimetry (ITC)

Experiments were performed using the iTC200 system (GE Healthcare) at 20°C with titration buffer (10 mM Hepes pH 7.8, 700mM NaCl, 1 mM MgCl2, 5% Glycerol, and 1mM DTT). 20 μM purified DCLK1 protein in 400ml of titration buffer was placed in the sample cell, and 200 μM compound in 40μl of titration buffer was loaded into the injection syringe. A 120-s delay at the start of the experiment was followed by 20 injections with 120-s intervals. All measured samples were stirred at 500 rpm. The data were analyzed in SEDPHAT and exported in GUSSI.

Western Blotting

Whole cell lysates were separated by SDS-PAGE gel and protein was transferred onto Immobilon-P membrane. The membrane was blocked by 5% milk in PBS with 0.1% Tween-20. The blot was probed with the DCLK1 antibody from Cell Signaling (Danvers, MA). Protein was detected by LumiGLO reagent and peroxide from Cell Signaling. Secondary antibody was from Cell Signaling.

Cell Proliferation Assay

CellTiter-Glo reagent was ordered from Promega (Madison, WI). Briefly, 50,000 cells were seeded per well in a 100 μl medium in 96-well format and were treated by a compound or transfected with a DNA construct. Assays were developed by addition of 100 μl of CellTiter-Glo reagent. Luminescence was measured using BioTek NEO plate reader.

Mass Spectrometry and Data Analysis

DLD-1 cells overexpressing DCLK1 were treated with 1 μM of DCLK1-IN-1 for 1, 4 and 24 hours. DMSO treatment at 4 hours was used as a control. After treatment, cells were harvested and were washed with cold PBS buffer for 3 times. Cells were harvested in ice-cold PBS. Quantitative mass spectrometry-based proteomics were performed as previously described (Biancur et al., 2017; Paulo et al., 2017). TMT isobaric reagents were from Thermo Scientific (909406, Life Technologies). Water and organic solvents were from J.T. Baker (Center Valley, PA, USA). Cell lysis was carried out in 2% SDS buffer with 25 mM NaCl, 20 mM HEPES pH 8.8, 5 mM dithiothreitol (DTT, to reduce disulfide bonds), 200 μM sodium orthovanadate (New England Biolabs, P0758S), and 1 × Halt™ Protease and Phosphatase Inhibitor Cocktail (Life Technologies, 78847) with zirconium oxide beads (Next Advance / MidSci ZROB05) using a vortexer at maximum speed for 5 min (Tissue Lyser LT, Qiagen). The homogenized cell lysate was placed at 60°C for 30 min, followed by cooling at room temperature for 10 min. Proteins were alkylated with 14 mM iodoacetamide (I1149 Sigma) at room temperature for 30 min in the dark. Excess iodoacetamide was quenched with 15 mM dithiothreitol at room temperature for 15 min in the dark.

Chloroform-methanol precipitation of proteins from cells was performed prior to protease digestion. To summarize, three parts neat methanol was added to each sample and vortexed, one part chloroform was added to the sample and vortexed, and 2.5 parts water was added to the sample and vortexed. The sample was centrifuged at 4000 × g for 10 min at room temperature and subsequently washed twice with 100% methanol. Samples were resuspended in 200 mM HEPES pH 8.5 for digestion. Protein concentrations were determined using the bicinchoninic acid (BCA) assay.

For each sample, 100 μg of protein was digested overnight with 1:100 protease-to-protein ratio Lys-C protease (129–02541, Wako Chemicals USA, Inc.) followed by trypsin (V5117, Promega) at a 1:100 protease-to-protein ratio, all at 37°C. Digested peptides were separated from contaminants using 50 mg silica bonded phase cartridges (WAT054960, Waters) followed by lyophilization using a speedvac concentrator overnight. 50 μg of peptides from each sample (as quantified using Micro BCA (Thermo Scientific, Rockford, IL)) were labelled with TMT reagent (100 μg) for 1 h, followed by quenching the reaction with hydroxylamine to a final concentration of 0.3% v/v. As a check to ensure effective labeling and appropriate ratios, we mixed 2% of each labeled sample in a 1:1:1:1:1:1:1:1:1:1:1:1:1:1:1:1 ratio and performed a ‘ratio check’ using LC/MS/MS. Based on ratios measured in this ratio check, we then combined the remainder of the samples. The combined sample was acidified, vacuum centrifuged to near dryness and subjected to C18 SPE (Sep-Pak, Waters). Next, each sample was enriched for phosphopeptides using the Pierce High-Select FE-NTA phosphopeptide Enrichment Kit following the manufacturer instructions. After phosphopeptide elution, the sample was lyophilized using a speedvac concentrator. For whole proteome analysis, the flow through from the phosphopeptide enrichment was collected and the sample was separated using basic pH reversed-phase HPLC and then pooled into 12 fractions. Data for the whole proteome and phosphoproteome analysis were obtained using an Orbitrap Fusion Lumos mass spectrometer (Thermo Fisher Scientific, San Jose, CA, USA) coupled with a Proxeon EASY-nLC 1200 LC pump (Thermo

Fisher Scientific). Peptides were separated on a 75 μm inner diameter microcapillary column packed with 35 cm of Accucore C18 resin (2.6 μm, 100 Å, Thermo Fisher Scientific). Peptides for global proteome analysis were separated using a 3 hour gradient of 6–27% acetonitrile in 0.125% formic acid with a flow rate of 400 nL/min. Phosphopeptides were analyzed using a 2 h gradient of 1–22% acetonitrile in 0.125% formic acid with a flow rate of 400 nL/min. The data were acquired using a mass range of m/z 350–1350, resolution 120,000, AGC target 1×10^6, maximum injection time 100 ms, dynamic exclusion of 120 s for the peptide measurements in the Orbitrap. Data dependent MS^2 spectra were acquired in the ion trap with a normalized collision energy (NCE) set at 35%, AGC target set to 1.8×10^4 and a maximum injection time of 120 ms. MS^3 scans were acquired in the Orbitrap with a HCD collision energy set to 55%, AGC target set to 1.5 X 10^5, maximum injection time of 150 ms, resolution at 50,000 and with a maximum synchronous precursor selection (SPS) precursors set to 10. Phosphopeptide data were acquired using the same parameters as described above with the addition of MultiStage Activation (MSA). Mass spectra were processed using a Sequest-based-in-house software pipeline as described previously (Paulo et al., 2015). Protein and phosphopeptide quantitation values were exported for further analysis. Each reporter ion channel was summed across all quantified proteins and normalized assuming equal protein loading in all 15 samples.

MS data analysis was previously reported (Lyons et al., 2018; Poulin et al., 2019). Briefly, we performed GSEA analysis on phosphoproteomic data with custom gene sets constructed of kinases and their respective species-specific substrate sites. Kinases were considered significantly active if the enrichment of their substrate set surpassed a threshold of either a nominal P-value < 0.05 or an FDR q value < 0.25.

QUANTIFICATION AND STATISTICAL ANALYSIS

One way ANOVA was used for comparisons with more than two groups. If there was a statistics difference, two-tail unpaired T test was used to compare each individual group. If not specified, the first sample was the control to make statistics analysis. * was used for $p < 0.05$ and ** was used for $p < 0.01$.

Supplementary Material

Refer to Web version on PubMed Central for supplementary material.

ACKNOWLEDGMENTS

We gratefully acknowledge Dr. Steven Gygi for use of CORE for mass spectrometry data analysis software. This research has been supported by a grant from the Hale Family Center for Pancreatic Cancer Research to J.D.M. and N.S.G. American Cancer Society Award 132205-RSG-18-039-01-DMC (to K.D.W.); Cancer Prevention and Research Institute of Texas RP170373 (to K.D.W); Welch Foundation Grant I1829 (to K.D.W.); 2017 AACR-Bayer Innovation and Discovery grant no. 17-80-44-GRAY (to N.S.G.); DF/HCC GI SPORE Developmental Research Project Award P50CA127003 (to N.S.G.); NIH grant 5U01CA207160 (to S.J.C., E.N.M., and A.T.); NIH U54-HL127365 and U24-DK116204 (to P.K.S.). We thank Samantha Westover for drawings in the graphical abstract. We thank Isabelle Lucet and colleagues for discussions regarding the G532V mutation.

REFERENCES

Ahmed RL, Shaughnessy DP, Knutson TP, Vogel RI, Ahmed K, Kren BT, and Trembley JH (2019). CDK11 loss induces cell cycle dysfunction and death of BRAF and NRAS melanoma cells. Pharmaceuticals (Basel) 12, 50.

Austin CA, and Marsh KL (1998). Eukaryotic DNA topoisomerase II beta. Bioessays 20, 215–226. [PubMed: 9631649]

Bailey JM, Alsina J, Rasheed ZA, McAllister FM, Fu YY, Plentz R, Zhang H, Pasricha PJ, Bardeesy N, Matsui W, et al. (2014). DCLK1 marks a morphologically distinct subpopulation of cells with stem cell properties in preinvasive pancreatic cancer. Gastroenterology 146, 245–256. [PubMed: 24096005]

Baumann G, Frommel C, and Sander C. (1989). Polarity as a criterion in protein design. Protein Eng. 2, 329–334. [PubMed: 2928295]

Biancur DE, Paulo JA, Malachowska B, Quiles Del Rey M, Sousa CM, Wang X, Sohn ASW, Chu GC, Gygi SP, Harper JW, et al. (2017). Compensatory metabolic networks in pancreatic cancers upon perturbation of glutamine metabolism. Nat. Commun. 8, 15965. [PubMed: 28671190]

Cancer Genome Atlas Research, N. (2014). Comprehensive molecular characterization of gastric adenocarcinoma. Nature 513, 202–209. [PubMed: 25079317]

Chandrakesan P, May R, Qu D, Weygant N, Taylor VE, Li JD, Ali N, Sureban SM, Qante M, Wang TC, et al. (2015). Dclk1+ small intestinal epithelial tuft cells display the hallmarks of quiescence and self-renewal. Oncotarget 6, 30876–30886. [PubMed: 26362399]

Chandrakesan P, Panneerselvam J, Qu D, Weygant N, May R, Bronze MS, and Houchen CW (2016). Regulatory roles of Dclk1 in epithelial mesenchymal transition and cancer stem cells. J. Carcinog. Mutagen 7, 257. [PubMed: 27335684]

Chandrakesan P, Weygant N, May R, Qu D, Chinthalapally HR, Sureban SM, Ali N, Lightfoot SA, Umar S, and Houchen CW (2014). DCLK1 facilitates intestinal tumor growth via enhancing pluripotency and epithelial mesenchymal transition. Oncotarget 5, 9269–9280. [PubMed: 25211188]

Chandrakesan P, Yao J, Qu D, May R, Weygant N, Ge Y, Ali N, Sureban SM, Gude M, Vega K, et al. (2017). Dclk1, a tumor stem cell marker, regulates pro-survival signaling and self-renewal of intestinal tumor cells. Mol. Cancer 16, 30. [PubMed: 28148261]

Chen H, Tucker J, Wang X, Gavine PR, Phillips C, Augustin MA, Schreiner P, Steinbacher S, Preston M, and Ogg D. (2016). Discovery of a novel allosteric inhibitor-binding site in ERK5: comparison with the canonical kinase hinge ATP-binding site. Acta Crystallogr. D Struct. Biol. 72, 682–693. [PubMed: 27139631]

Deng X, Dzamko N, Prescott A, Davies P, Liu Q, Yang Q, Lee JD, Patricelli MP, Nomanbhoy TK, Alessi DR, et al. (2011a). Characterization of a selective inhibitor of the Parkinson's disease kinase LRRK2. Nat. Chem. Biol. 7, 203–205. [PubMed: 21378983]

Deng X, Yang Q, Kwiatkowski N, Sim T, McDermott U, Settleman JE, Lee JD, and Gray NS (2011b). Discovery of a benzo[e]pyrimido-[5,4-b][1,4] diazepin-6(11H)-one as a potent and selective inhibitor of big MAP kinase 1. ACS Med. Chem. Lett. 2, 195–200. [PubMed: 21412406]

Ferguson F, Nabet B, Raghavan S, Liu Y, Leggett A, Kuljanin M, Kalekar R, Yang A, He S, Wang J, et al. (2020). Discovery of a selective inhibitor of doublecortin like kinase 1. Nat. Chem. Biol. 16, 635–643. [PubMed: 32251410]

Ferguson FM, Doctor ZM, Chaikuad A, Sim T, Kim ND, Knapp S, and Gray NS (2017). Characterization of a highly selective inhibitor of the Aurora kinases. Bioorg. Med. Chem. Lett. 27, 4405–4408. [PubMed: 28818446]

Gagliardi G, Goswami M, Passera R, and Bellows CF (2012). DCLK1 immunoreactivity in colorectal neoplasia. Clin. Exp. Gastroenterol. 5, 35–42. [PubMed: 22557932]

Gao T, Wang M, Xu L, Wen T, Liu J, and An G. (2016). DCLK1 is up-regulated and associated with metastasis and prognosis in colorectal cancer. J. Cancer Res. Clin. Oncol. 142, 2131–2140. [PubMed: 27520310]

Gilsbach BK, Messias AC, Ito G, Sattler M, Alessi DR, Wittinghofer A, and Kortholt A. (2015). Structural characterization of LRRK2 inhibitors. J. Med. Chem. 58, 3751–3756. [PubMed: 25897865]

Hafner M, Niepel M, Chung M, and Sorger PK (2016). Growth rate inhibition metrics correct for confounders in measuring sensitivity to cancer drugs. Nat. Methods 13, 521–527. [PubMed: 27135972]

Hoelder S, Clarke PA, and Workman P. (2012). Discovery of small molecule cancer drugs: successes, challenges and opportunities. Mol. Oncol. 6, 155–176. [PubMed: 22440008]

Hu D, Mayeda A, Trembley JH, Lahti JM, and Kidd VJ (2003). CDK11 complexes promote pre-mRNA splicing. J. Biol. Chem. 278, 8623–8629. [PubMed: 12501247]

Ikezono Y, Koga H, Akiba J, Abe M, Yoshida T, Wada F, Nakamura T, Iwamoto H, Masuda A, Sakaue T, et al. (2017). Pancreatic neuroendocrine tumors and EMT behavior are driven by the CSC marker DCLK1. Mol. Cancer Res. 15, 744–752. [PubMed: 28179411]

Ito H, Tanaka S, Akiyama Y, Shimada S, Adikrisna R, Matsumura S, Aihara A, Mitsunori Y, Ban D, Ochiai T, et al. (2016). Dominant expression of DCLK1 in human pancreatic cancer stem cells accelerates tumor invasion and metastasis. PLoS One 11, e0146564.

Jafari R, Almqvist H, Axelsson H, Ignatushchenko M, Lundback T, Nordlund P, and Martinez Molina D. (2014). The cellular thermal shift assay for evaluating drug target interactions in cells. Nat. Protoc. 9, 2100–2122. [PubMed: 25101824]

Johnson JO, Pioro EP, Boehringer A, Chia R, Feit H, Renton AE, Pliner HA, Abramzon Y, Marangi G, Winborn BJ, et al. (2014). Mutations in the Matrin 3 gene cause familial amyotrophic lateral sclerosis. Nat. Neurosci. 17, 664–666. [PubMed: 24686783]

Kadletz L, Aumayr K, Heiduschka G, Schneider S, Enzenhofer E, and Lill C. (2017). Overexpression of DCLK1 is predictive for recurrent disease in major salivary gland malignancies. Eur. Arch. Otorhinolaryngol. 274, 467–475. [PubMed: 27470117]

Koga H, Ikezono Y, and Torimura T. (2016). Pancreatic DCLK1 marks quiescent but oncogenic progenitors: a possible link to neuroendocrine tumors. Stem Cell Investig. 3, 37.

Koizumi H, Fujioka H, Togashi K, Thompson J, Yates JR 3rd, Gleeson JG, and Emoto K. (2017). DCLK1 phosphorylates the microtubule-associated protein MAP7D1 to promote axon elongation in cortical neurons. Dev. Neurobiol. 77, 493–510.

Lenart P, Petronczki M, Steegmaier M, Di Fiore B, Lipp JJ, Hoffmann M, Rettig WJ, Kraut N, and Peters JM (2007). The small-molecule inhibitor BI 2536 reveals novel insights into mitotic roles of polo-like kinase 1. Curr. Biol. 17, 304–315. [PubMed: 17291761]

Lim SM, Xie T, Westover KD, Ficarro SB, Tae HS, Gurbani D, Sim T, Marto JA, Janne PA, Crews CM, et al. (2015). Development of small molecules targeting the pseudokinase Her3. Bioorg. Med. Chem. Lett. 25, 3382–3389. [PubMed: 26094118]

Lin A, Giuliano CJ, Palladino A, John KM, Abramowicz C, Yuan ML, Sausville EL, Lukow DA, Liu L, Chait AR, et al. (2019). Off-target toxicity is a common mechanism of action of cancer drugs undergoing clinical trials. Sci. Transl. Med. 11, eaaw8412.

Lin PT, Gleeson JG, Corbo JC, Flanagan L, and Walsh CA (2000). DCAMKL1 encodes a protein kinase with homology to doublecortin that regulates microtubule polymerization. J. Neurosci. 20, 9152–9161. [PubMed: 11124993]

Lipka J, Kapitein LC, Jaworski J, and Hoogenraad CC (2016). Microtubule-binding protein doublecortin-like kinase 1 (DCLK1) guides kinesin-3-mediated cargo transport to dendrites. EMBO J. 35, 302–318. [PubMed: 26758546]

Liu JS, Schubert CR, Fu X, Fourniol FJ, Jaiswal JK, Houdusse A, Stultz CM, Moores CA, and Walsh CA (2012). Molecular basis for specific regulation of neuronal kinesin-3 motors by doublecortin family proteins. Mol. Cell 47, 707–721. [PubMed: 22857951]

Liu W, Wang S, Sun Q, Yang Z, Liu M, and Tang H. (2018). DCLK1 promotes epithelial-mesenchymal transition via the PI3K/Akt/NF-kappaB pathway in colorectal cancer. Int. J. Cancer 142, 2068–2079. [PubMed: 29277893]

Lu Y, Maruyama J, Kuwata K, Fukuda H, Iwasa H, Arimoto-Matsuzaki K, Sugimura H, and Hata Y. (2018). Doublecortin-like kinase 1 compromises DNA repair and induces chromosomal instability. Biochem. Biophys. Rep. 16, 130–137. [PubMed: 30417131]

Lyons J, Brubaker DK, Ghazi PC, Baldwin KR, Edwards A, Boukhali M, Strasser SD, Suarez-Lopez L, Lin YJ, Yajnik V, et al. (2018). Integrated in vivo multiomics analysis identifies p21-activated kinase signaling as a driver of colitis. Sci. Signal. 11, eaan3580.

Lyu YL, and Wang JC (2003). Aberrant lamination in the cerebral cortex of mouse embryos lacking DNA topoisomerase IIbeta. Proc. Natl. Acad. Sci. U S A 100, 7123–7128. [PubMed: 12773624]

Malik AM, Miguez RA, Li X, Ho YS, Feldman EL, and Barmada SJ (2018). Matrin 3-dependent neurotoxicity is modified by nucleic acid binding and nucleocytoplasmic localization. eLife 7, e35977.

May R, Qu D, Weygant N, Chandrakesan P, Ali N, Lightfoot SA, Li L, Sureban SM, and Houchen CW (2014). Brief report: Dclk1 deletion in tuft cells results in impaired epithelial repair after radiation injury. Stem Cells 32, 822–827. [PubMed: 24123696]

McClendon AK, and Osheroff N. (2007). DNA topoisomerase II, genotoxicity, and cancer. Mutat. Research-Fundamental Mol. Mech. Mutagenesis 623, 83–97.

McMillan EA, Ryu MJ, Diep CH, Mendiratta S, Clemenceau JR, Vaden RM, Kim JH, Motoyaji T, Covington KR, Peyton M, et al. (2018). Chemistry-first approach for nomination of personalized treatment in lung cancer. Cell 173, 864–878.e9.

Mizuguchi M, Qin J, Yamada M, Ikeda K, and Takashima S. (1999). High expression of doublecortin and KIAA0369 protein in fetal brain suggests their specific role in neuronal migration. Am. J. Pathol. 155, 1713–1721. [PubMed: 10550327]

Mohammadi Y, Tavangar SM, Saidijam M, Amini R, Etemadi K, Karimi Dermani F, and Najafi R. (2018). DCLK1 plays an important role in colorectal cancer tumorgenesis through the regulation of miR-200c. Biomed. Pharmacother. 103, 301–307. [PubMed: 29656186]

Nakanishi Y, Seno H, Fukuoka A, Ueo T, Yamaga Y, Maruno T, Nakanishi N, Kanda K, Komekado H, Kawada M, et al. (2013). Dclk1 distinguishes between tumor and normal stem cells in the intestine. Nat. Genet. 45, 98–U143. [PubMed: 23202126]

Patel O, Dai W, Mentzel M, Griffin MD, Serindoux J, Gay Y, Fischer S, Sterle S, Kropp A, Burns CJ, et al. (2016). Biochemical and structural insights into doublecortin-like kinase domain 1. Structure 24, 1550–1561. [PubMed: 27545623]

Paulo JA, O'Connell JD, Gaun A, and Gygi SP (2015). Proteome-wide quantitative multiplexed profiling of protein expression: carbon-source dependency in Saccharomyces cerevisiae. Mol. Biol. Cell 26, 4063–4074. [PubMed: 26399295]

Paulo JA, Mancias JD, and Gygi SP (2017). Proteome-wide protein expression profiling across five pancreatic cell lines. Pancreas 46, 690–698. [PubMed: 28375945]

Poulin EJ, Bera AK, Lu J, Lin Y-J, Strasser SD, Paulo JA, Huang TQ, Morales C, Yan W, Cook J, et al. (2019). Tissue-specific oncogenic activity of KRASA146T. Cancer Discov. 9, 738–755. [PubMed: 30952657]

Powrozek T, Krawczyk P, Nicos M, Kuznar-Kaminska B, Batura-Gabryel H, and Milanowski J. (2016). Methylation of the DCLK1 promoter region in circulating free DNA and its prognostic value in lung cancer patients. Clin. Transl Oncol. 18, 398–404. [PubMed: 26311076]

Qu D, May R, Sureban SM, Weygant N, Chandrakesan P, Ali N, Li L, Barrett T, and Houchen CW (2014). Inhibition of Notch signaling reduces the number of surviving Dclk1+ reserve crypt epithelial stem cells following radiation injury. Am. J. Physiol. Gastrointest. Liver Physiol. 306, G404–G411. [PubMed: 24368703]

Rangarajan P, Subramaniam D, Paul S, Kwatra D, Palaniyandi K, Islam S, Harihar S, Ramalingam S, Gutheil W, Putty S, et al. (2015). Crocetinic acid inhibits hedgehog signaling to inhibit pancreatic cancer stem cells. Oncotarget 6, 27661–27673. [PubMed: 26317547]

Reiner O, Coquelle FM, Peter B, Levy T, Kaplan A, Sapir T, Orr I, Barkai N, Eichele G, and Bergmann S. (2006). The evolving doublecortin (DCX) superfamily. BMC Genomics 7, 188. [PubMed: 16869982]

Richards FM (1977). Areas, volumes, packing and protein structure. Annu. Rev. Biophys. Bioeng. 6, 151–176. [PubMed: 326146]

Sakaguchi M, Hisamori S, Oshima N, Sato F, Shimono Y, and Sakai Y. (2016). miR-137 regulates the tumorigenicity of colon cancer stem cells through the inhibition of DCLK1. Mol. Cancer Res. 14, 354–362. [PubMed: 26747706]

Salton M, Elkon R, Borodina T, Davydov A, Yaspo ML, Halperin E, and Shiloh Y. (2011). Matrin 3 binds and stabilizes mRNA. PLoS One 6, e23882. [PubMed: 21858232]

Shaheen S, Ahmed M, Lorenzi F, and Nateri AS (2016). Spheroid-formation (colonosphere) assay for in vitro assessment and expansion of stem cells in colon cancer. Stem Cell Rev. Rep. 12, 492–499. [PubMed: 27207017]

Shin E, Kashiwagi Y, Kuriu T, Iwasaki H, Tanaka T, Koizumi H, Gleeson JG, and Okabe S. (2013). Doublecortin-like kinase enhances dendritic remodelling and negatively regulates synapse maturation. Nat. Commun. 4, 1440. [PubMed: 23385585]

Sossey-Alaoui K, and Srivastava AK (1999). DCAMKL1, a brain-specific transmembrane protein on 13q12.3 that is similar to doublecortin (DCX). Genomics 56, 121–126. [PubMed: 10036192]

Steegmaier M, Hoffmann M, Baum A, Lenart P, Petronczki M, Krssak M, Gurtler U, Garin-Chesa P, Lieb S, Quant J, et al. (2007). BI 2536, a potent and selective inhibitor of polo-like kinase 1, inhibits tumor growth in vivo. Curr. Biol. 17, 316–322. [PubMed: 17291758]

Suehiro Y, Takemoto Y, Nishimoto A, Ueno K, Shirasawa B, Tanaka T, Kugimiya N, Suga A, Harada E, and Hamano K. (2018). Dclk1 inhibition cancels 5-FU-induced cell-cycle arrest and decreases cell survival in colorectal cancer. Anticancer Res. 38, 6225–6230. [PubMed: 30396941]

Sureban SM, Madhoun MF, May R, Qu D, Ali N, Fazili J, Weygant N, Chandrakesan P, Ding K, Lightfoot SA, et al. (2015). Plasma DCLK1 is a marker of hepatocellular carcinoma (HCC): targeting DCLK1 prevents HCC tumor xenograft growth via a microRNA-dependent mechanism. Oncotarget 6, 37200–37215. [PubMed: 26468984]

Sureban SM, May R, Qu D, Weygant N, Chandrakesan P, Ali N, Lightfoot SA, Pantazis P, Rao CV, Postier RG, et al. (2013). DCLK1 regulates pluripotency and angiogenic factors via microRNA-dependent mechanisms in pancreatic cancer. PLoS One 8, e73940.

Sureban SM, May R, Weygant N, Qu D, Chandrakesan P, BannermanMenson E, Ali N, Pantazis P, Westphalen CB, Wang TC, et al. (2014). XMD8–92 inhibits pancreatic tumor xenograft growth via a DCLK1-dependent mechanism. Cancer Lett. 351, 151–161. [PubMed: 24880079]

Vedeld HM, Skotheim RI, Lothe RA, and Lind GE (2014). The recently suggested intestinal cancer stem cell marker DCLK1 is an epigenetic biomarker for colorectal cancer. Epigenetics 9, 346–350. [PubMed: 24384857]

Verissimo CS, Molenaar JJ, Meerman J, Puigvert JC, Lamers F, Koster J, Danen EH, van de Water B, Versteeg R, Fitzsimons CP, et al. (2010). Silencing of the microtubule-associated proteins doublecortinlike and doublecortin-like kinase-long induces apoptosis in neuroblastoma cells. Endocr. Relat. Cancer 17, 399–414. [PubMed: 20228126]

Verissimo CS, Cheng S, Puigvert JC, Qin Y, Vroon A, van Deutekom J, Price LS, Danen EH, van de Water B, Fitzsimons CP, et al. (2012). Combining doublecortin-like kinase silencing and vinca alkaloids results in a synergistic apoptotic effect in neuroblastoma cells. J. Pharmacol. Exp. Ther. 342, 119–130. [PubMed: 22490379]

Wang K, Yuen ST, Xu J, Lee SP, Yan HH, Shi ST, Siu HC, Deng S, Chu KM, Law S, et al. (2014). Whole-genome sequencing and comprehensive molecular profiling identify new driver mutations in gastric cancer. Nat. Genet. 46, 573–582. [PubMed: 24816253]

Wang W, Zhang H, Wang L, Zhang S, and Tang M. (2016). miR613 inhibits the growth and invasiveness of human hepatocellular carcinoma via targeting DCLK1. Biochem. Biophys. Res. Commun. 473, 987–992. [PubMed: 27049311]

Westphalen CB, Quante M, and Wang TC (2017). Functional implication of Dclk1 and Dclk1-expressing cells in cancer. Small GTPases 8, 164–171. [PubMed: 27458755]

Westphalen CB, Takemoto Y, Tanaka T, Macchini M, Jiang Z, Renz BW, Chen X, Ormanns S, Nagar K, Tailor Y, et al. (2016). Dclk1 defines quiescent pancreatic progenitors that promote injury-induced regeneration and tumorigenesis. Cell Stem Cell 18, 441–455. [PubMed: 27058937]

Weygant N, Ge Y, Qu D, Kaddis JS, Berry WL, May R, Chandrakesan P, Bannerman-Menson E, Vega KJ, Tomasek JJ, et al. (2016). Survival of patients with gastrointestinal cancers can be predicted by a surrogate microRNA signature for cancer stem-like cells marked by DCLK1 kinase. Cancer Res. 76, 4090–4099. [PubMed: 27287716]

Weygant N, Qu D, Berry WL, May R, Chandrakesan P, Owen DB, Sureban SM, Ali N, Janknecht R, and Houchen CW (2014). Small molecule kinase inhibitor LRRK2-IN-1 demonstrates potent

activity against colorectal and pancreatic cancer through inhibition of doublecortin-like kinase 1. Mol. Cancer 13, 103. [PubMed: 24885928]

Weygant N, Qu D, May R, Tierney RM, Berry WL, Zhao L, Agarwal S, Chandrakesan P, Chinthalapally HR, Murphy NT, et al. (2015). DCLK1 is a broadly dysregulated target against epithelial-mesenchymal transition, focal adhesion, and stemness in clear cell renal carcinoma. Oncotarget 6, 2193–2205. [PubMed: 25605241]

Whorton J, Sureban SM, May R, Qu D, Lightfoot SA, Madhoun M, Johnson M, Tierney WM, Maple JT, Vega KJ, et al. (2015). DCLK1 is detectable in plasma of patients with Barrett's esophagus and esophageal adenocarcinoma. Dig. Dis. Sci. 60, 509–513. [PubMed: 25283374]

Williamson DS, Smith GP, Acheson-Dossang P, Bedford ST, Chell V, Chen IJ, Daechsel JCA, Daniels Z, David L, Dokurno P, et al. (2017). Design of leucine-rich repeat kinase 2 (LRRK2) inhibitors using a crystallographic surrogate derived from checkpoint kinase 1 (CHK1). J. Med. Chem. 60, 8945–8962. [PubMed: 29023112]

Wu X, Qu D, Weygant N, Peng J, and Houchen CW (2020). Cancer stem cell marker DCLK1 correlates with tumorigenic immune infiltrates in the colon and gastric adenocarcinoma microenvironments. Cancers (Basel) 12, 274.

Xie T, Lim SM, Westover KD, Dodge ME, Ercan D, Ficarro SB, Udayakumar D, Gurbani D, Tae HS, Riddle SM, et al. (2014). Pharmacological targeting of the pseudokinase Her3. Nat. Chem. Biol. 10, 1006–1012. [PubMed: 25326665]

Yang X. (2000). DNA topoisomerase II and neural development. Science 287, 131–134. [PubMed: 10615047]

Zhou Y, Han C, Li D, Yu Z, Li F, Li F, An Q, Bai H, Zhang X, Duan Z, et al. (2015). Cyclin-dependent kinase 11(p110) (CDK11(p110)) is crucial for human breast cancer cell proliferation and growth. Sci. Rep. 5, 10433. [PubMed: 25990212]

Zhou Y, Shen JK, Hornicek FJ, Kan Q, and Duan Z. (2016). The emerging roles and therapeutic potential of cyclin-dependent kinase 11 (CDK11) in human cancer. Oncotarget 7, 40846–40859. [PubMed: 27049727]

Highlights

- Overexpression or DCLK1 in DLD-1 cells results in DCLK1-dependent growth
- Genetic or chemical ablation of DCLK1 activity inhibits DCLK1-transformed cell growth
- The DCLK1 mutation G532A results in DCLK1-IN-1-resistance
- DCLK1 inhibition decreases RNA processing and other cellular processes

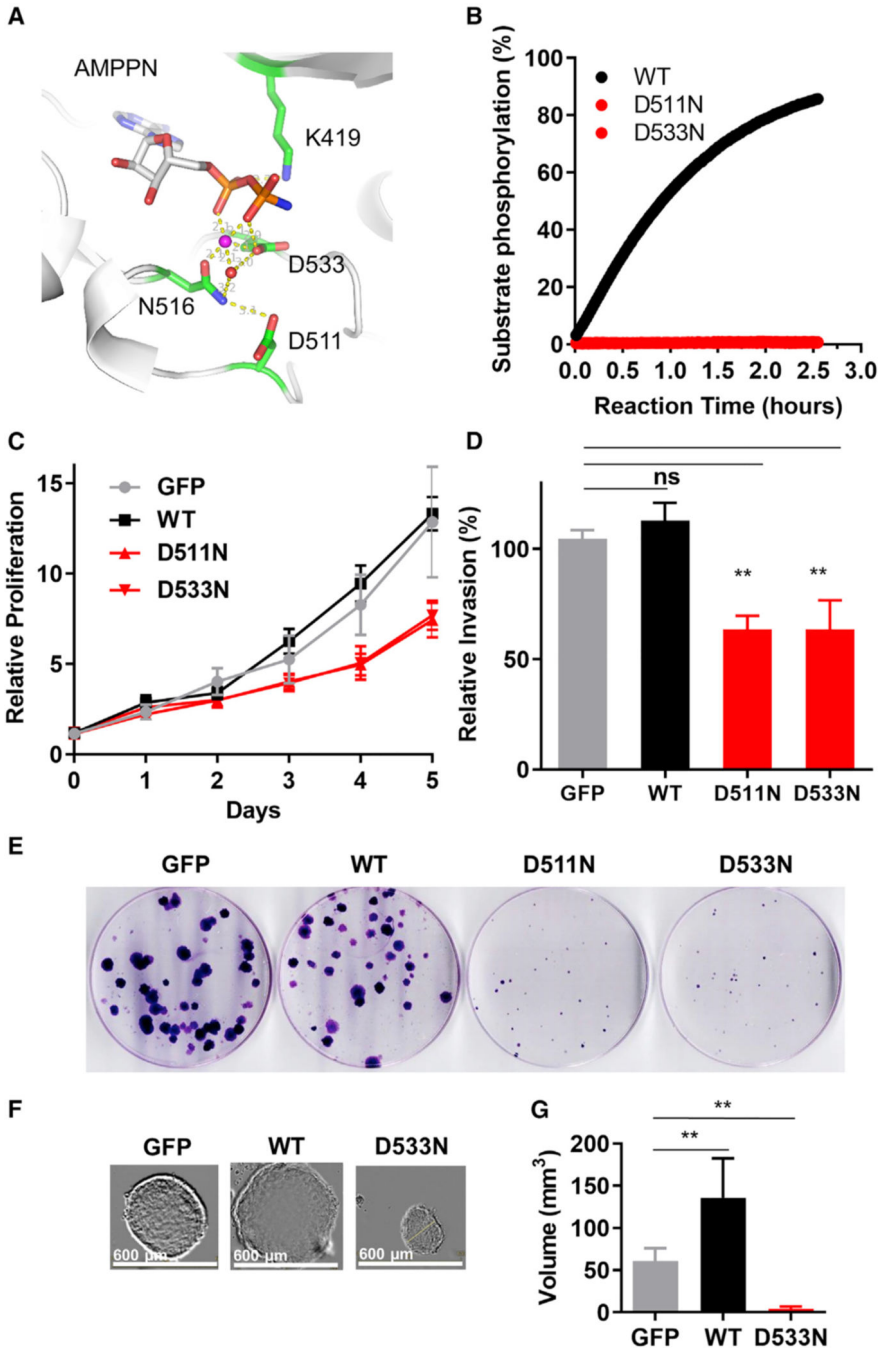

Figure 1. Ablation of DCLK1 Kinase Activity Disrupts the Malignant Behavior of DLD-1 Cells

(A) Catalytic residues in DCLK1 kinase active site (PDB: 5JZN). AMPPN is an ADP analog.

(B) D511N or D533N extinguished DCLK1 kinase activity. Activity was measured by peptide substrate mobility shift assay.

(C) Proliferation of DLD-1 cells was not altered by stable overexpression of WT DCLK1, but was reduced by DCLK1-KD D511N or D533N.

(D) Cell invasion of DLD-1 was impaired by overexpression of DCLK1-KD. Results are normalized to GFP control.
(E) Colony-forming ability of DLD-1 cells was impaired in DCLK1-KD mutants.
(F) Spheroid assays showed profound growth defects in DLD-1 cells expressing DCLK1-KD. Scale bars, 600 μm.
(G) Quantitation of spheroid volume shown as the average of at least three samples.
For all panels error bars are the SD. **$p < 0.01$.

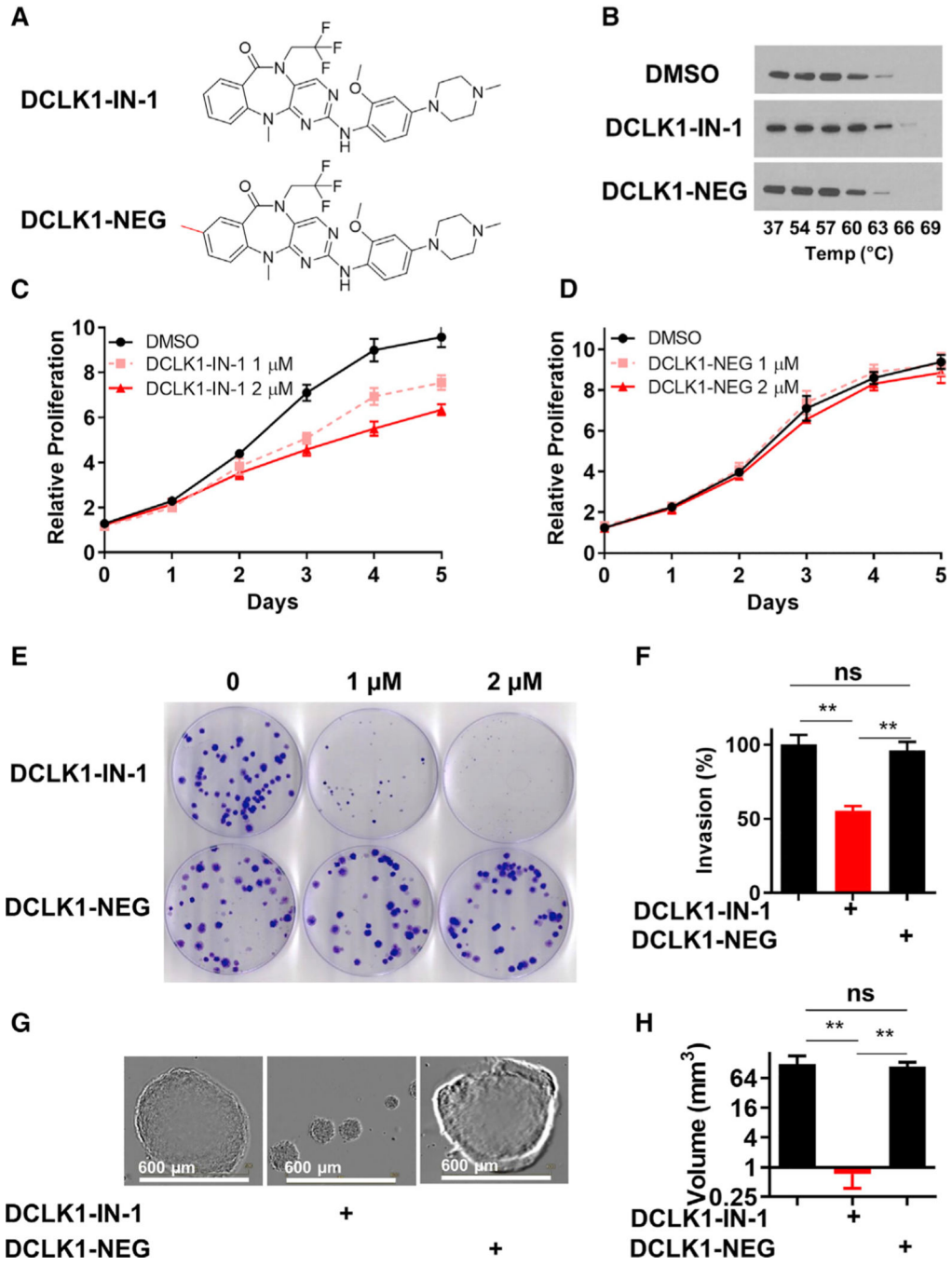

Figure 2. The DCLK1 Inhibitor DCLK1-IN-1 Phenocopies DCLK1-KD

(A) Chemical structures of DCLK1-IN-1 and the negative control DCLK1-NEG.

(B) Cellular thermal shift assay confirmed target engagement by DCLK1-IN-1 but not DCLK1-NEG in DLD-1 cells overexpressing WT DCLK1.

(C and D) Cell proliferation of DLD-1 overexpressing WT DCLK1 was reduced by DCLK1-IN-1 but not by DCLK1-NEG.

(E) Colony-forming ability of DLD-1 overexpressing WT DCLK1 was determined when treated with DCLK1-IN-1 or DCLK1-NEG for 1 week. Cells were stained by crystal violet solution.

(F) Treatment with 1 μM of DCLK1-IN-1, but not DCLK1-NEG, resulted in loss of cell invasion in DLD-1 cells overexpressing WT DCLK1. Results were normalized to DMSO control.

(G) Spheroid assays showed that treatment with 1 μM of DCLK1-IN-1, but not DCLK1-NEG, led to growth defects in DLD-1 cells overexpressing WT DCLK1.

(H) Quantitation of spheroid volume.

For all panels error bars were the SD. ** $p < 0.01$.

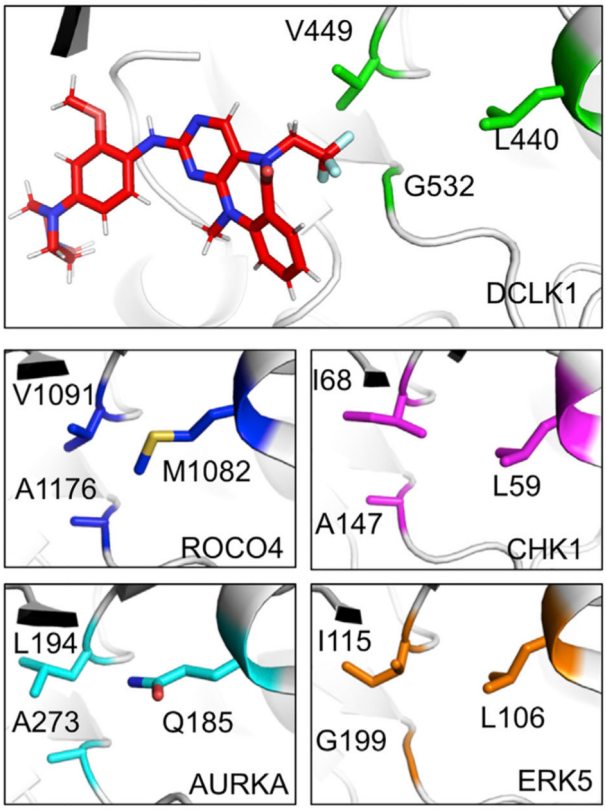

B

Kinase	Residue position			Side chain volume (Å^3)
	440	449	532	
DCLK1	L	V	G	376
AURK	Q	L	A	421
CHK1	L	I	A	429
ERK5	L	I	G	403
ROCO4	M	V	A	405

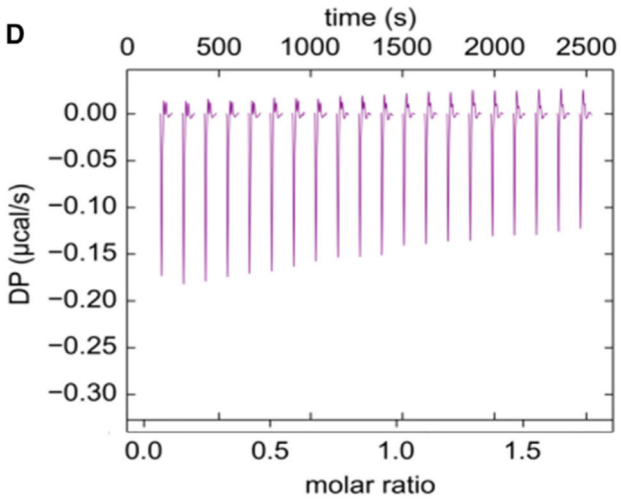

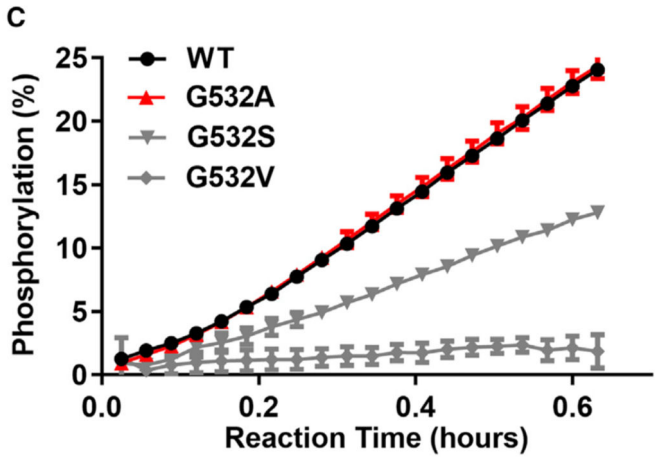

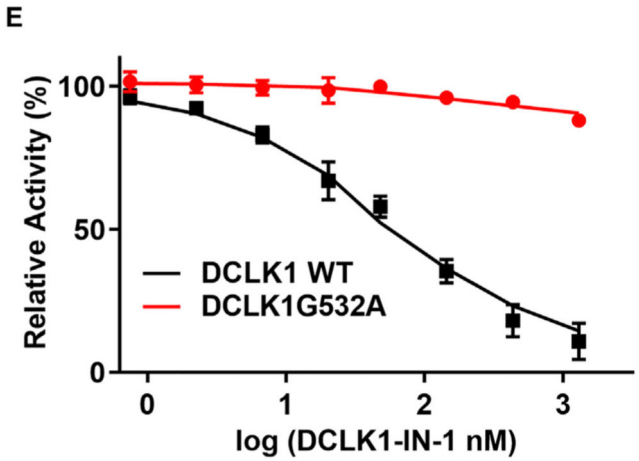

Figure 3. DCLK1 G532A Confers DCLK1-IN-1 Resistance

(A) Residues surrounding the binding pocket for the trifluoro substituent in DCLK1 include L440, V449, and G532. Corresponding residues in other kinases known to bind the core scaffold, but not trifluoro-containing analogs such as DCLK1-IN-1, also shown below.

(B) Calculation of the volume of side chains lining the trifluoro pocket showed that side-chain volume was smallest for DCLK1, suggesting that addition of side-chain volume in that region would lead to drug resistance.

(C) G532A was tolerated with respect to DCLK1 kinase activity. Other candidate mutations, DCLK1 G532S and DCLK1 G532V, showed a decrease in kinase activity as measured by peptide substrate mobility shift assay.
(D) Isothermal titration calorimetry showed loss of binding of DCLK1 G532A for DCLK1-IN-1. The molar ratio refers to the molecular ratio of DCLK1-IN-1 to DCLK1 protein molecules.
(E) DCLK1 G532A resulted in profound loss of inhibitory activity of DCLK1-IN-1.
For all panels error bars indicate the SD.

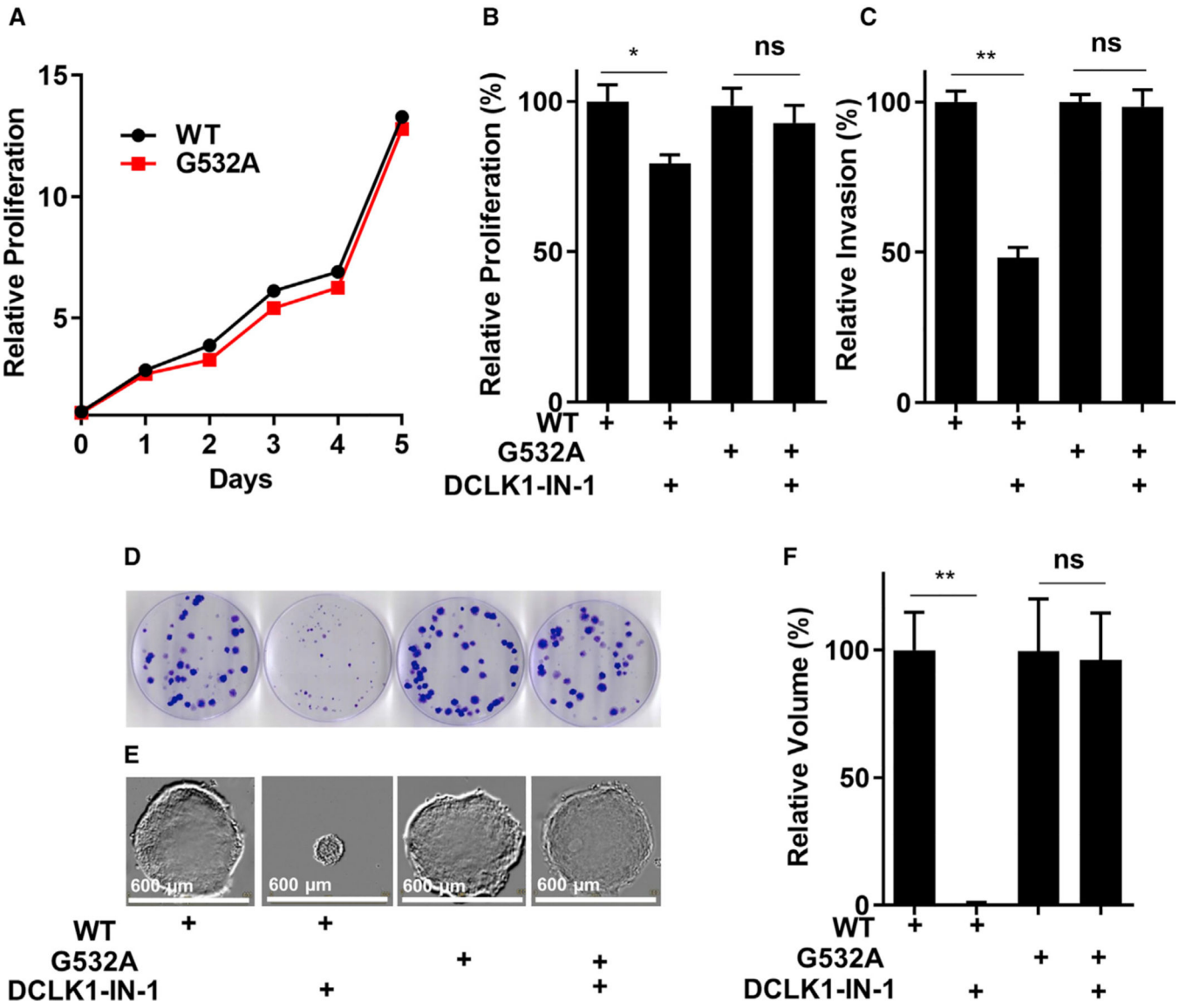

Figure 4. Overexpression of DCLK1 G532A Rescues DLD-1 Cells Exposed to DCLK1-IN-1

(A) G532A did not change cell proliferation relative to WT DCLK1.

(B) Inhibitory effects of DCLK1-IN-1 on cell proliferation were lost with G532A. Growth was assessed at 48 h. Results are normalized to DMSO control.

(C–E) (C) G532A rescued cells from DCLK1-IN-1-dependent effects on cell invasion. Cells were pretreated with 1 μM DCLK1-IN-1 for 24 h. Normalization was to GFP-expressing cells treated with DMSO. (D–E) G532A rescued colony-forming ability (D) and spheroid formation of DLD-1 cells overexpressing WT DCLK1 in the setting of 1 μM DCLK1-IN-1 (E).

(F) Quantitation of spheroids from (E). Scale bars, 600 μm. For all panels error bars indicate the SD.

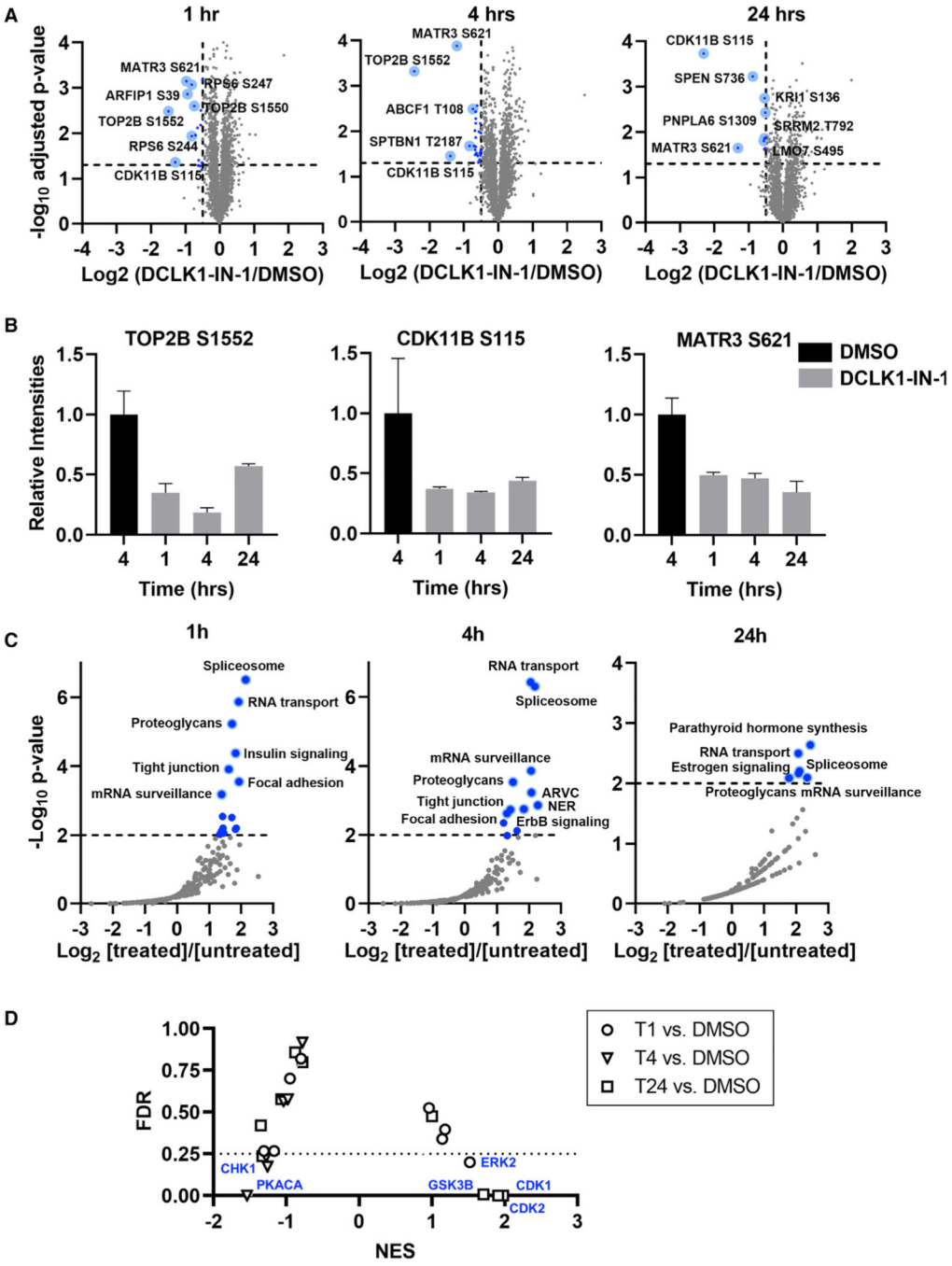

Figure 5. Quantitative DCLK1-IN-1 Phosphoproteomics in DLD-1 Cells Overexpressing WT DCLK1 Identifies Substrates of and Biological Associations with DCLK1

(A) Change in levels of phosphopeptide abundance for mean of DCLK1-IN-1 treated versus mean of DMSO-treated samples at three time points. Blue circles represent significantly downregulated phosphopeptides ($\log_2$(fold change) < −0.5, adjusted $p < 0.05$). Data shown are averaged from three biological replicates.

(B) Relative phosphorylated peptide MS intensity of the top three DCLK1 substrates over time. The levels of phosphorylated peptides were normalized to un-phosphorylated peptide

within each sample then the ratio for treated versus DMSO control was calculated. For all panels error bars are the SD.

(C) Kyoto Encyclopedia of Genes and Genomes analysis of MS data identified coordinated enrichment of spliceosome, RNA transport, insulin signaling, proteoglycans, mRNA surveillance, focal adhesion, and tight junction pathways in response to DCLK-IN-1 treatment at 1 and 4 h. RNA-related pathways persisted at 24 h.

(D) Changes in inferred kinase activity upon treatment with DCLK1-IN-1 identifies kinases that were potentially regulated by DCLK1. Plot shows association between normalized enrichment score (NES) and false discovery rate (FDR). Kinases with positive or negative enrichment and an FDR <0.25 are labeled.

Table 1.

Potential Substrates of DCLK1

Gene symbol	Site Position	Fold Change (Log2)	p Value (−Log10)
1 h DCLK1-IN-1 versus DMSO			
TOP2B	S1552	−1.49	2.48
CDK11B	S115	−1.30	1.36
MATR3	S621	−0.98	3.15
ARFIP1	S39	−0.94	2.86
RPS6	S244; S247	−0.82	1.93
TOP2B	S1550	−0.74	2.60
ECM29	S833	−0.71	1.95
SERBP1	S391	−0.65	2.12
4 h DCLK1-IN-1 versus DMSO			
TOP2B	S1552	−2.44	3.32
CDK11B	S115	−1.39	1.45
MATR3	S621	−1.20	3.88
SPTBN1	T2187	−0.84	1.67
ABCF1	T108; S109	−0.73	2.49
LMNA	S404; S407	−0.70	1.67
SPTBN1	T2328	−0.68	2.01
MAP1S	S731	−0.67	1.59
24 h DCLK1-IN-1 versus DMSO			
SPEN	S736; S740	−2.31	3.73
MATR3	S621	−1.31	1.64
CDK11B	S115	−0.88	3.22
PNPLA6	S1309; S1318	−0.56	1.80
LMO7	S495	−0.54	1.86
SRRM2	S2412	−0.54	1.62
KRI1	S136	−0.54	2.74
SLC9A1	S599; S602; T603	−0.53	1.64

De-enriched phosphorylated peptides in DLD-1 cells treated with DCLK1-IN-1 relative to 4 h DMSO control.

KEY RESOURCES TABLE

REAGENT or RESOURCE	SOURCE	IDENTIFIER
Antibodies		
Anti-DCLK1	Cell Signaling	Cat #62257; RRID: AB_2799622
Anti-GAPHD	Cell Signaling	Cat #5174; RRID: AB_10622025
Bacterial and Virus Strains		
E.coli BL21	New England Biolabs	Cat #C2527I
E.coli DH5α	New England Biolabs	Cat #C2988J
Chemicals, Peptides, and Recombinant Proteins		
DCLK1-IN-1	Gray Lab, Dana-Farber Cancer Institute	
DCLK1-NEG	Gray Lab, Dana-Farber Cancer Institute	
FL-Peptide 12: 5-FAM-KKLRRTLSVA-COOH	Caliper Life Science	
Critical Commercial Assays		
CellTiter-Glo reagent	Promega	Cat #G7570
Experimental Models: Cell Lines		
Human: DLD-1 cells	ATCC	CCL-221
Human: 184A1 cells	ATCC	CRL-8798; RRID CVCL_3040
Human:184B5 cells	ATCC	CRL-8799; RRID CVCL_4688
Human: AU565 cells	ATCC	CRL-2351; RRID CVCL_1074
Human: BT20 cells	ATCC	HTB-19; RRID CVCL_0178
Human: BT474 cells	ATCC	HTB-20; RRID CVCL_0179
Human:BT549 cells	ATCC	HTB-122; RRID CVCL_1092
Human: CAL120 cells	DSMZ	ACC 459; RRID CVCL_1104
Human: CAL51 cells	DSMZ	ACC 302; RRID CVCL_1110
Human:CAL851 cells	DSMZ	ACC 440; RRID CVCL_1114
Human: CAMA1 cells	ATCC	HTB-21; RRID CVCL_1115
Human: EFM19 cells	DSMZ	ACC 231; RRID CVCL_0253

REAGENT or RESOURCE	SOURCE	IDENTIFIER
Human: EVSAT cells	DSMZ	ACC 433; RRID CVCL_1207
Human: HCC1143 cells	ATCC	CRL-2321; RRID CVCL_1245
Human: HCC1395 cells	ATCC	CRL-2324; RRID CVCL_1249
Human: HCC1419 cells	ATCC	CRL-2326; RRID CVCL_1251
Human: HCC1569 cells	ATCC	CRL-2330; RRID CVCL_1255
Human: HCC1806 cells	ATCC	CRL-2335; RRID CVCL_1258
Human: HCC1937 cells	ATCC	CRL-2336; RRID CVCL_0290
Human: HCC1954 cells	ATCC	CRL-2338; RRID CVCL_1259
Human: HCC202 cells	ATCC	CRL-2316; RRID CVCL_2062
Human: HCC38 cells	ATCC	CRL-2314; RRID CVCL_1267
Human: HCC70 cells	ATCC	CRL-2315; RRID CVCL_1270
Human: HS578T cells	ATCC	HTB-126; RRID CVCL_0332
Human: HTERT_HME1 cells	ATCC	CRL-4010; RRID CVCL_3383
Human: MCF10A cells	ATCC	CRL-10317; RRID CVCL_0598
Human: MCF-12A cells	ATCC	CRL-10782; RRID CVCL_3744
Human: MDA-MB-175-VII cells	ATCC	HTB-25; RRID CVCL_1400
Human: MDA-MB-231 cells	ATCC	HTB-26; RRID CVCL_0062
Human: MDA-MB-330-cells	ATCC	HTB-127; RRID CVCL_0619
Human: MDA-MB-361cells	ATCC	HTB-27; RRID CVCL_0620
Human: MDA-MB-415 cells	ATCC	HTB-128; RRID CVCL_0621
Human: MDA-MB-436 cells	ATCC	HTB-130; RRID CVCL_0623
Human: MDA-MB-453 cells	ATCC	HTB-131; RRID CVCL_0418
Human: MDA-MB-468 cells	ATCC	HTB-132; RRID CVCL_0419
Human: SKBR3 cells	ATCC	HTB-30; RRID CVCL_0033
Human: SUM1315 cells	University of Michigan	SUM-1315MO2; RRID CVCL_5589
Human: SUM149 cells	Asterand	SUM-149PT; RRID CVCL_3422
Human: SUM159 cells	Asterand	SUM-159PT; RRID CVCL_54
Human: SUM185PE cells	Asterand	SUM-185PE; RRID CVCL_5591
Human: SUM229PE cells	Asterand	SUM-229PE; RRID CVCL_5594

REAGENT or RESOURCE	SOURCE	IDENTIFIER
Human: SUM52PE cells	Asterand	SUM-52PE; RRID CVCL_3425
Human: T47D cells	ATCC	HTB-133; RRID CVCL_0553
Human: UACC-812 cells	ATCC	CRL-1897; RRID CVCL_1781
Human: UACC-893 cells	ATCC	CRL-1902; RRID CVCL_1782
Human: ZR-75–1 cells	ATCC	CRL-1500; RRID CVCL_0588
Human: ZR-75–30 cells	ATCC	CRL-1504; RRID CVCL_1661
Recombinant DNA		
DCLK1 kinase domain DNA construct	Dr. Ana Clara Redondo University of Oxford	
pLenti6.3/v5-DCLK1 D511N	Westover Lab University of Texas Southwestern Medical Center at Dallas	
pLenti6.3/v5-DCLK1 D533N	Westover Lab University of Texas Southwestern Medical Center at Dallas	
pLenti6.3/v5-DCLK1 G532A	Westover Lab University of Texas Southwestern Medical Center at Dallas	
Software and Algorithms		
Prism8	GraphPad	
ImageJ		https://imagej.nih.gov/ij/